ISSN 1674-1056
http://cpb.iphy.ac.cn
http://iopscience.iop.org/cpb
中国物理 B
Chinese Physics
中国物理 Chinese Physics B

Phase diagram characterized by transmission in a triangular quantum dot

Jin Huang(黄金), Wei-Zhong Wang(王为忠)

Citation: Chin. Phys. B . 2018, 27(11): 117303. **doi:** 10.1088/1674-1056/27/11/117303

Journal homepage: http://cpb.iphy.ac.cn; http://iopscience.iop.org/cpb

What follows is a list of articles you may be interested in

Enhanced transient photovoltaic characteristics of core-shell ZnSe/ZnS/L-Cys quantum-dot-sensitized TiO_2 thin-film

Kui-Ying Li(李葵英), Lun Ren(任伦), Tong-De Shen(沈同德)

Chin. Phys. B . 2018, 27(6): 067305. **doi:** 10.1088/1674-1056/27/6/067305

Optical anisotropy and the direction of polarization of exciton emissions in a semiconductor quantum dot:Effect of heavy- and light-hole mixing

Ranber Singh, Rajiv Kumar, Vikramjeet Singh

Chin. Phys. B . 2017, 26(8): 087303. **doi:** 10.1088/1674-1056/26/8/087303

Spin-dependent thermoelectric effect and spin battery mechanism in triple quantum dots with Rashba spin-orbital interaction

Wei-Ping Xu(徐卫平), Yu-Ying Zhang(张玉颖), Qiang Wang(王强), Yi-Hang Nie(聂一行)

Chin. Phys. B . 2016, 25(11): 117307. **doi:** 10.1088/1674-1056/25/11/117307

Carrier transport in III-V quantum-dot structures for solar cells or photodetectors

Wenqi Wang(王文奇), Lu Wang(王禄), Yang Jiang(江洋), Ziguang Ma(马紫光), Ling Sun(孙令), Jie Liu(刘洁), Qingling Sun(孙庆灵), Bin Zhao(赵斌), Wenxin Wang(王文新), Wuming Liu(刘伍明), Haiqiang Jia(贾海强), Hong Chen(陈弘)

Chin. Phys. B . 2016, 25(9): 097307. **doi:** 10.1088/1674-1056/25/9/097307

Majorana fermion realization and relevant transport processes in a triple-quantum dot system

Deng Ming-Xun, Zheng Shi-Han, Yang Mou, Hu Liang-Bin, Wang Rui-Qiang

Chin. Phys. B . 2015, 24(3): 037302. **doi:** 10.1088/1674-1056/24/3/037302

Phase diagram characterized by transmission in a triangular quantum dot*

Jin Huang(黄金) and Wei-Zhong Wang(王为忠)†

Department of Physics, Wuhan University, Wuhan 430072, China

(Received 20 June 2018; revised manuscript received 5 September 2018; published online 25 October 2018)

We propose a theoretical model to detect the quantum phase transition in a triangular quantum dot molecule with frustration. The boundaries of the phase diagram are accurately determined by the transmission. For small frustration t, as the interdot Coulomb repulsion V increases, the system undergoes a Kosterlitz–Thouless (KT) transition from the Kondo resonance state with a transmission peak at zero energy to the Coulomb blocked state with zero transmission, which is followed by a first transition to the V-induced resonance (VIR) state with unitary transmission. For large frustration t, as V increases, the orbital spin singlet without transmission transits to the VIR state through a KT transition.

Keywords: quantum dots, quantum phase transition, Kondo effect, transmission

PACS: 73.63.–b, 71.27.+a, 72.15.Qm **DOI:** 10.1088/1674-1056/27/11/117303

1. Introduction

In contrast to bulk materials, artificial quantum dots (QDs) exhibit large tunability of quantum states and are ideal nanoscale devices to observe quantum phase transitions (QPTs). Although QPTs of different kinds have been predicted in coupled double quantum dot (DQD) and triple quantum dot (TQD) systems,[1–14] only a few have been experimentally demonstrated. For instance, as interdot coupling increases, a continuous transition from a single-peak Kondo resonance state to a double-peak state has been observed in a DQD fabricated on a GaAs heterostructures.[15] In C_{60} single-molecule QD, the singlet–triplet QPT is achieved by tuning the gate voltage.[16] Generally, the quantum critical phenomenon related to a zero-temperature QPT is characterized by the behaviors of charge and spin correlations, which cannot be directly observed in the experiment. It is therefore desirable to explore the QPT through detecting the transport properties, such as conductance, transmission, and susceptibility. In this paper, we propose a theoretical model for a triangular TQD system with frustration. The complicated phase diagram can be obtained by analyzing the behavior of the transmission.

Experimentally, the TQD systems have been realized in semiconductor heterostructures and self-assembled systems.[17–23] According to different research goals, various configurations of quantum dots and leads can be fabricated. The triangular TQD is the simplest system with a closed loop which causes quantum interference effect and frustration. The interplay between the strong correlation and interdot hopping plays an important role in manipulating the spin–spin interaction and electronic transport.

Theoretically, the triangular TQD systems have been studied by several groups. For triangular cluster of three spin-1/2 Kondo or Anderson impurities connected in series to two leads, a crossover between a Fermi-liquid and non-Fermi-liquid has been found when the interdot exchange interactions or interdot hopping changes.[24] For a similar model with two-channel environment, a frustration-induced QPT is driven by varying the interdot exchange coupling.[25] For the configuration with one metallic lead to four leads, the Kondo physics, the low-energy properties, and the amplitude leakage phenomenon have been investigated.[26–29]

All these studies focus on the interplay between the on-site Coulomb repulsion U and the interdot tunnel couplings. In this paper, we consider a triangular TQD molecule with two dots connected to leads, as shown in Fig. 1. The geometrical frustration can destroy the symmetry in the triangular TQD. The interplay between the on-site Hubbard repulsion U, the interdot Coulomb repulsion V, and the frustration t results in a complicated phase diagram. For small V and without the frustration t, each dot is singly occupied due to the Hubbard interaction U and three dots form a spin doublet, which is screened by the metallic leads and is accompanied with the Kondo resonance (KR) at low temperature. As V increases, the system undergoes a Kosterlitz–Thouless (KT) transition to a Coulomb blockade (CB) state at the first critical point $V = V_{c1}$, followed by a first order transition to a V-induced resonance (VIR) state at the second critical point $V = V_{c2}$. For small V, as t increases, there exists a first order transition from the KR state to an orbital spin singlet (OSS), in which the even orbital is doubly occupied and forms an orbital spin singlet. For larger V, as t increases, we find the CB–VIR transition of first order at t_{c1} and the VIR–OSS transition of the KT type. The phase boundary can be characterized by the transmission spectra $T(\omega)$. For instance, at the KR–OSS transition point, the Kondo resonance

*Project supported by the National Natural Science Foundation of China (Grant Nos. 11174228 and 10874132).

†Corresponding author. E-mail: wzwang@whu.edu.cn

© 2018 Chinese Physical Society and IOP Publishing Ltd

peak disappears on the side of the OSS state. Along the two KT transition lines, the width of the transmission peak depends exponentially on the distance to the critical point. In the CB regime, we observe two CB peaks while in the VIR regime the transmission with unitary limit recovers. Since the transmission can be conveniently obtained by the experiment, we believe this characteristic provides a possibility to experimentally demonstrate the QPT in a TQD system.

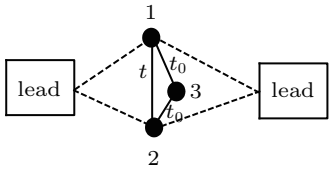


Fig. 1. Triangular quantum dots attached to the leads. t_0 and t denote the interdot hopping.

2. The model and calculation methods

We consider a triangular TQD system shown in Fig. 1. Dots 1 and 2 connect to the leads, and each dot is coupled to the others. Both the on-site and the interdot Coulomb repulsions are taken into account. The Hamiltonian is described as

$$\begin{aligned} H &= \sum_{jk\sigma} \epsilon_k c^{\dagger}_{jk\sigma} c_{jk\sigma} + \sum_{jk\sigma} V_k c^{\dagger}_{jk\sigma}(d_{1\sigma} + d_{2\sigma}) + \text{H.c.} \\ &\quad + \epsilon \sum_i d^{\dagger}_{i\sigma} d_{i\sigma} + U \sum_i n_{i\uparrow} n_{i\downarrow} + V \sum_{i<j} n_i n_j \\ &\quad - \sum_{ij} t_{ij} (d^{\dagger}_{i\sigma} d_{j\sigma} + \text{H.c.}). \end{aligned} \tag{1}$$

Here, $d^{\dagger}_{i\sigma}$ and $c^{\dagger}_{jk\sigma}$ are the dot and lead creation operators, respectively, $n_{i\sigma} = d^{\dagger}_{i\sigma} d_{i\sigma}$ and $n_i = n_{i\uparrow} + n_{i\downarrow}$, ϵ and ϵ_k are orbital energies on the dots and leads, respectively, $t_{13} = t_{23} = t_0$ and $t_{12} = t$ are interdot hoppings, U and V are the on-site and interdot Coulomb repulsions, respectively, and V_k is the tunnel matrix element between leads and dots.

We calculate the electronic transport using the numerical renormalization-group method (NRG).[30,31] We assume a dispersionless conduction band with a half bandwidth D and a constant density of state ρ_0. The tunnel coupling between dots and the leads $\Gamma = 2\pi\rho_0|V_k|^2$ is taken as a constant. In our NRG calculation, the discretization parameter is $\Lambda = 1.5 - 2.5$, and the number of the states kept at each iteration is between 1300 and 2000. We apply a new procedure to evaluate the Green function with respect to the reduced density matrix of the full system, which is demonstrated to lead to accurate spectra.[32] The linear conductance at zero temperature in the limit of zero bias is determined by

$$G = \frac{2e^2}{h} T(\omega = 0), \tag{2}$$

with the transmission coefficient

$$T(\omega) = -\frac{1}{2}\Gamma \sum_{ij\sigma} \text{Im} G_{ij\sigma}(\omega). \tag{3}$$

Here the retarded dot Green function is defined as $G_{ij\sigma}(t) = -i\theta(t)\langle\{d_{i\sigma}(t), d^{\dagger}_{j\sigma}\}\rangle$.

3. Results and discussions

We present the phase diagram on the $t-V$ plane in Fig. 2. For small frustration t, with V increasing, the system transits from the Kondo resonance state to the Coulomb blockade state, then to the V-induced resonance state. For large t, the system enters into the orbital spin singlet state. In the following, we determine the nature of the phase transitions and describe the characteristics of different phases. We find that the phase boundary can be characterized by the transmission spectra $T(\omega)$. We focus on the effect of the interdot repulsion V and the frustration t on the QPT and transport properties. In this paper, the half bandwidth D of the leads is taken as the energy unit. We focus on the strongly correlated regime and take $\Gamma = 0.01$, $U = 0.1$, $\epsilon = -U/2 - 2V$, and $t_0 = 0.01$.

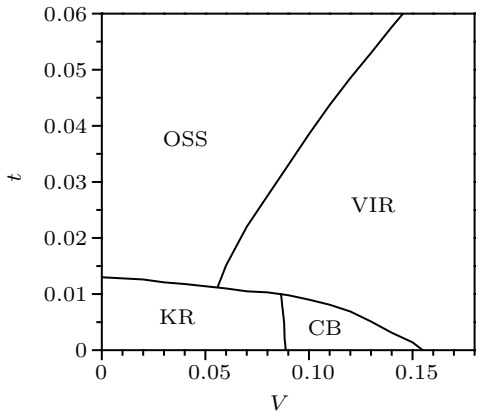


Fig. 2. Phase diagram on the t–V plane indicates the Kondo resonance state, the Coulomb blockade state, V-induced resonance state, and the orbital spin singlet. Here, $\Gamma = 0.01$, $U = 0.1$, $t_0 = 0.01$, and $\epsilon = -U/2 - 2V$.

3.1. Without frustration for $t = 0$

First, we study the QPT for $t = 0$. In this case, the system is a bipartite system without frustration and has the particle–hole symmetry at $\epsilon = -U/2 - 2V$. Because the Fermi level is chosen as $\epsilon_{k_F} = 0$ in the NRG calculation, the TQD system is half filled and the electron occupation in each dot is always $n_i = 1$ at $\epsilon = -U/2 - 2V$.

For small V, each dot tends to be singly occupied due to the strong on-site Coulomb repulsion U. There are antiferromagnetic interactions between dot 3, dot 1, and dot 2 due to the interdot hopping t_0 and the on-site Coulomb repulsion U. Therefore, the TQD forms a local doublet with a local spin $S_{\text{dot}} = 1/2$. At low temperature, this local spin is totally screened by the conduction electrons in the leads, and the Kondo effect is observed. Figure 3 shows the transmission $T(\omega)$ at zero temperature for different V values. For small V in Fig. 3(a), one can see a Kondo resonance peak, correspond-

ing to the full conductance $G = 2e^2/h$, and a Coulomb peak at about $\omega = \pm U/2$.

The interdot Coulomb repulsion V is favorable for the dots doubly occupied and it can destroy the Kondo resonance. As V increases, the width of the Kondo peak becomes narrow (e.g., $V = 0.062$ in Fig. 3(a)). This indicates that the Kondo effect occurs at lower temperature. When V is larger than a critical $V_{c1} = 0.0888$ (e.g., $V = 0.12$ in Fig. 3(b)), the Kondo peak disappears and the Coulomb peak is located at about $\omega = \pm(V - U/2)$. This behavior indicates that at $V = V_{c1}$, there is a transition from the Kondo resonance state to the Coulomb blockade state. To explore the characteristic of the QPT, we present the transmission $T(\omega)$ in Fig. 4(a) in the regime $V < V_{c1}$ and close to the critical point V_{c1}. We find that the width of Kondo peak W depends exponentially on the distance to the critical point $(V - V_{c1})$ and can be adequately described using an exponential function $W = C\exp[-A/(V - V_{c2})^{\nu}]$, where the fitting parameters $C = 1.0002$, $A = 1.9513$, and $\nu = 0.4370$. Figure 4(b) indicates that the fitting function (solid line) agrees very well with the NRG results (scattering dots). This exponentially-dependent width W indicates that the KR–CB transition at V_{c1} is a QPT of the KT type.[33]

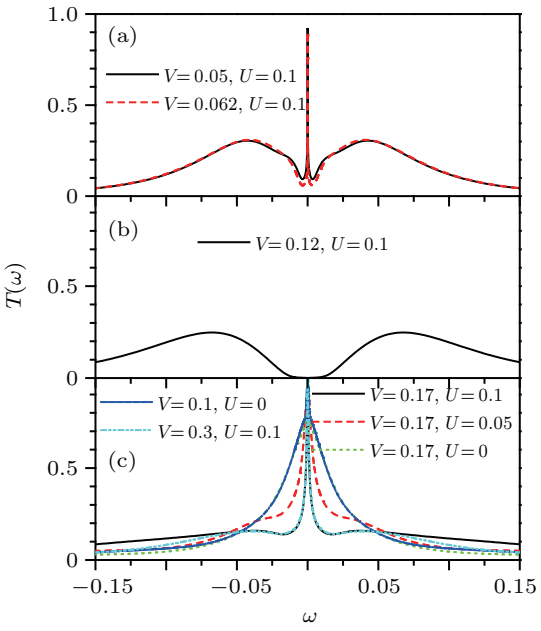


Fig. 3. (color online) Transmission coefficient $T(\omega)$ at zero temperature for different V and U values. Here, $\Gamma = 0.01$, $t_0 = 0.01$, $t = 0$, and $\epsilon = -U/2 - 2V$.

As V increases to the second critical point $V_{c2} = 0.154$ (e.g., $V = 0.17$ in Fig. 3(c)), we also observe a transmission $T(\omega = 0)$ with a unitary limit. We call this ground state as the V-induced resonance state. The shape of the transmission spectra does not depend on V in the VIR state. For instance, the curves for different V and the same U coincide with each other; although with U increasing, the peak becomes narrow. This feature is quite different from the above KR in Fig. 3(b). In order to explain this behavior of the transmission, we introduce the combinations of the dot orbitals; i.e., $f_{1\sigma} = (d_{1\sigma} + d_{2\sigma})/\sqrt{2}$, $f_{2\sigma} = (d_{1\sigma} - d_{2\sigma})/\sqrt{2}$, and $f_{3\sigma} = d_{3\sigma}$. Under this transformation, the interaction terms in the dot Hamiltonian in Eq. (4) can be expressed as

$$\begin{aligned} H_{\rm dot}^{\rm int} = & \frac{1}{2}(U+V)(n'_{1\uparrow}+n'_{2\uparrow})(n'_{1\downarrow}+n'_{2\downarrow}) + V(n'_{1\uparrow}n'_{2\uparrow}+n'_{1\downarrow}n'_{2\downarrow}) \\ & + \frac{1}{2}(U-V)(f^{\dagger}_{1\uparrow}f_{2\uparrow}+f^{\dagger}_{2\uparrow}f_{1\uparrow})(f^{\dagger}_{1\downarrow}f_{2\downarrow}+f^{\dagger}_{2\downarrow}f_{1\downarrow}) \\ & + Un'_{3\uparrow}n'_{3\downarrow} + V(n'_1+n'_2)n'_3, \end{aligned} \tag{4}$$

where $n'_{i\sigma} = f^{\dagger}_{i\sigma}f_{i\sigma}$ and $n'_i = n'_{i\uparrow} + n'_{i\downarrow}$. In this case, the leads are just connected to the orbital $f_{1\sigma}$ with even parity. According to Eq. (3), the transmission $T(\omega)$ is merely determined by the density of state of orbital $f_{1\sigma}$.

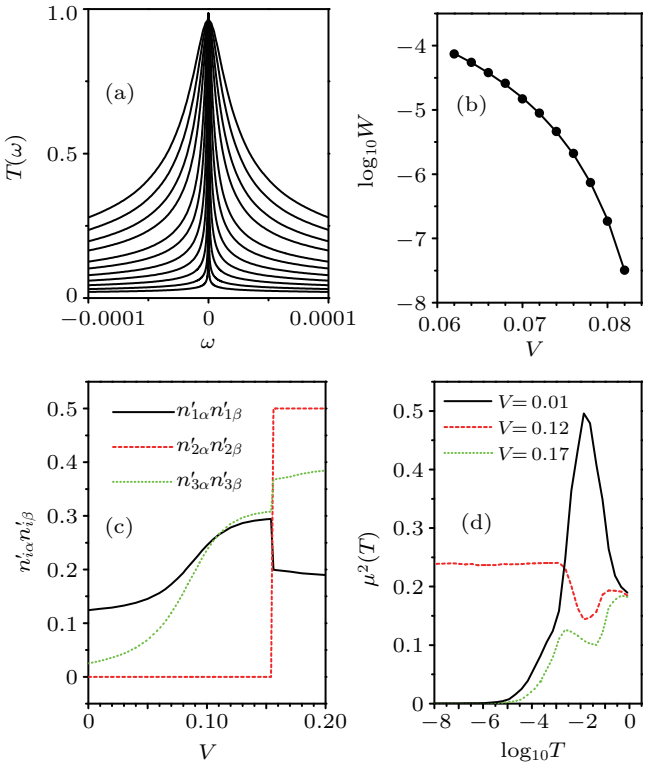


Fig. 4. (color online) (a) Transmission $T(\omega)$ in the KR state near the critical point $V = V_{c1}$; the curves from top to bottom are for V=0.062 to 0.082 in steps of 0.002. (b) The width of the Kondo peak W (scattering dots) and its stimulant exponential function (solid line) as a function of V near V_{c1}. (c) Double occupation $\langle n'_{i\uparrow}n'_{i\downarrow}\rangle$ on the transformed orbital $f_{i\sigma}$ as a function of V. (d) Total magnetic moment $\mu^2(T)$ as a function of the temperature T for different V values. Here, $U = 0.1$ and the remaining parameters are the same as in Fig. 3.

We show the double occupation $\langle n'_{i\uparrow}n'_{i\downarrow}\rangle$ in Fig. 4(c). As V increases, the double occupation $\langle n'_{1\uparrow}n'_{1\downarrow}\rangle$ on dot 1 increases from about 0.12 at $V = 0$ to about 0.30 at $V = 0.15$. It is known that the double occupation for a half-filled noninteraction orbital is 1/4. The Kondo effect requires the dot to be almost singly occupied. As a result, the Kondo resonance can not be observed for large V. Meanwhile, according to Eqs. (4) and

(1), one can deduce that for large V, adding an additional electron to the system will cost energy $V-U/2$. Therefore, the CB peaks appear at $\omega=\pm(V-U/2)$ as shown in Fig. 3(b). The continuous change of $\langle n'_{i\uparrow}n'_{i\downarrow}\rangle$ at the critical $V=V_{c1}$ indicates that the transition from the KR state to the CB state is continuous.

As $V>V_{c2}$, there is an abrupt change of the double occupation $\langle n'_{i\uparrow}n'_{i\downarrow}\rangle$ (see Fig. 4(c)). In particular, the double occupation $\langle n'_{2\uparrow}n'_{2\downarrow}\rangle$ on the orbital $f_{2\sigma}$ increases from 0 to 0.5, which indicates that the orbital $f_{2\sigma}$ is doubly occupied or empty. Meanwhile, the double occupation on the orbital $f_{1\sigma}$ decreases to $\langle n'_{1\uparrow}n'_{1\downarrow}\rangle\approx 0.2$, which is smaller than 0.25 of the double occupation on a half-filled non-interaction orbital. According to Eq. (3), after the transformation of dot orbitals, the transmission $T(\omega)$ is determined by the single occupation on orbital $f_{1\sigma}$. The increase of the single occupation on the orbital $f_{1\sigma}$ induces a transmission $T(\omega=0)$ with a unitary limit in the VIR state.

Figure 4(d) shows the temperature dependence of the total magnetic moment defined by $\mu^2(T)=\langle S_z^2\rangle-\langle S_z^2\rangle_0$, where $\langle S_z^2\rangle$ and $\langle S_z^2\rangle_0$ denote the thermodynamic expectation values of the square of the z component of the total spin of the system with and without quantum dots, respectively.[30,31] For small V (e.g., $V=0.01$), at a high temperature $T\sim 0.015$, each dot has a free local spin 1/2 and contributes 1/4 to μ^2. Because there is some possibility of double occupy in this regime, μ^2 is about 0.5 which is smaller than the maximum 3/4. With T decreasing (e.g., $T\sim 0.001<4t_0^2/U$), the interdot antiferromagnetic interactions drive the triple dots to a doublet with $\mu^2\approx 1/4$. At lower temperature $T\to 0$, the local spin $S_{\rm dot}=1/2$ is totally screened by the conduction electron in the leads and a Kondo resonance is observed in Fig. 3(a). For $V>V_{c1}$ (e.g., $V=0.12$), the double occupation on the transformed orbitals $f_{1\sigma}$ and $f_{3\sigma}$ is large (see Fig. 4(c)) while the orbital $f_{2\sigma}$ is still singly occupied. As a result, no local spin on the orbital $f_{1\sigma}$ can be screened by the conduction electron in the leads. We observe a residual magnetic moment $\mu^2=0.25$ in the CB state, which is the local spin on the orbital $f_{2\sigma}$.

Although we observe the full conductance both in the KR state and the VIR state in Fig. 3, their origins are quite different. For small V in Fig. 3(a), the spin of the electron on a singly occupied orbital $f_{1\sigma}$ is screened by the conduction electron in the leads. Therefore, adding an additional electron with opposite spin to this orbital does not require overcoming the on-site Coulomb repulsion U. This is the so called Kondo effect. However, for large V in Fig. 3(c), the full conductance does not mainly result from the screening effect of the spin on the dot. For instance, even for on-site repulsion $U=0$ we still observe a perfect transmission $T(\omega=0)=1$ in Fig. 3(c). From Eqs. (1) and (4), one finds that adding an electron to the singly occupied dot orbital $f_{1\sigma}$ requires energy $\epsilon+2V=0$ equal to the Fermi energy and, therefore, the electron can transmit the dot freely. For $U=0$, transmission spectra $T(\omega)$ are given by a Lorentzian with a width 2Γ. With U increasing (e.g., $U=0.05$ and 0.1 in Fig. 3(c)), $T(\omega)$ becomes narrow rapidly. This feature can be explained by the following picture. As U increases, there is a small antiferromagnetic interaction between the dots and the leads. This antiferromagnetic interaction induces a small magnetic moment μ^2 of about 0.13 at temperature $T\sim 0.002$ (e.g., for $U=0.1$ and $V=0.17$ in Fig. 4(d)). At lower temperature $T\to 0$, this magnetic moment is screened by the conduction electron in the leads. According to Haldane's expression,[30,31] the screening temperature $T_{\rm K}$ decreases exponentially as U/Γ increases, corresponding to the width of the transmission spectrum. The calculation shows that as U increases, the transmission spectrum changes from the Lorentzian to the sharp peak smoothly. This feature indicates that in the VIR ground state, although the on-site repulsion U affects the shape of the transmission spectrum, the origin of the full conductance is the same as that for $U=0$ and $V>0$. As U increases to a critical $U_c>V$, the system transits to the CB state in Fig. 3(b). From Fig. 3(c), we also find that the shape of the transmission spectra does not depend on V in the VIR state. For instance, the curves for different V and the same U coincide with each other. This feature is quite different from the Kondo resonance induced by the on-site repulsion U.

3.2. Effect of the frustration for $t\neq 0$

Next, we consider the TQD system with frustration t. For nonzero interdot hopping t, the particle–hole symmetry is broken due to the frustration. The electron occupation in each dot $n_i=1$ is not kept at $\epsilon=-U/2-2V$. From the phase diagram in Fig. 2, we can see that for small V and large V, the phase sequences are quite different.

For small V (e.g., $V=0.05$), Figs. 5(a) and 5(b) show the transmission $T(\omega)$ at zero temperature for different t. For small frustration t (e.g., $t=0.0114$ in Fig. 5(a)), the Coulomb peaks at $\omega\approx\pm U/2$ and the Kondo resonance peak at $\omega=0$ are still observed. The ground state is the KR state. As t is greater than the critical $t_c=0.01147$ (e.g., $t=0.0115$ in Fig. 5(b)), the Kondo peak disappears and the Coulomb peaks move to the direction $\omega<0$, which indicates an increase of the occupation on the orbital $f_{1\sigma}$. In order to understand this behavior, we give the energy levels of the even orbital $f_{1\sigma}$ and the odd orbital $f_{2\sigma}$ as $\epsilon_1=\epsilon-t$ and $\epsilon_2=\epsilon+t$. Obviously, as t increases, ϵ_1 decreases while ϵ_2 increases. Figures 5(c) and 5(d) show the charge occupation n'_i and the double occupation $\langle n'_{i\uparrow}n'_{i\downarrow}\rangle$ on each orbital. It is found that the orbital $f_{1\sigma}$ is almost doubly occupied for large $t>t_c$ while $f_{3\sigma}$ is singly occupied and $f_{2\sigma}$ is nearly empty. In this case, the Hamiltonian in Eq. (1) maps to a single impurity Anderson model with

impurity orbital $f_{1\sigma}$ connected to the leads while the singly occupied $f_{3\sigma}$ and the empty orbital $f_{2\sigma}$ decouple from $f_{1\sigma}$. Because the impurity orbital $f_{1\sigma}$ is doubly occupied, the electrons on $f_{1\sigma}$ form an orbital spin-singlet (OSS) without Kondo effect.

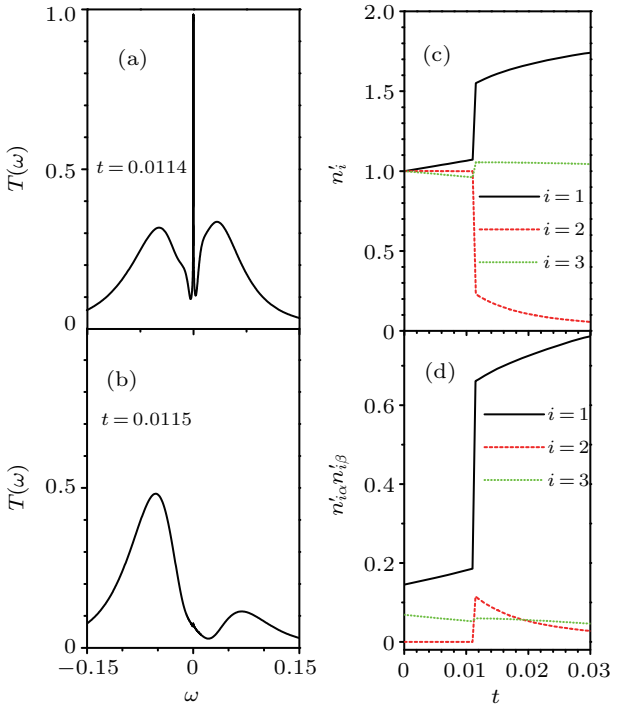


Fig. 5. (color online) (a) and (b) Transmission $T(\omega)$ for different t values. (c) Charge occupation n'_i and (d) double occupation $\langle n'_{i\uparrow}n'_{i\downarrow}\rangle$ on orbital $f_{i\sigma}$ as a function of t. Here, $\Gamma = 0.01$, $t_0 = 0.01$, $U = 0.1$, $V = 0.05$, and $\epsilon = -U/2 - 2V$.

For large V (e.g., $V = 0.12$), the transmission $T(\omega)$ in Fig. 6 exhibits two kinds of phase transitions. For small t, the system is in the CB state (Fig. 6(a)) although the two Coulomb peaks are not symmetric about $\omega = 0$ due to the frustration. As t is greater than a critical value $t_{c1} = 0.00683$ (e.g., $t = 0.0069$ in Fig. 6(b)), the system transits to the VIR state with a sharp central peak and a full conductance. With further increase of t, the peak becomes narrow and disappears at $t = t_{c2} = 0.0457$ (e.g., $t = 0.05$ in Fig. 6(c)). This feature indicates that there is phase transition from the VIR state to the OSS state. Figure 7(a) shows the critical behavior of the transmission on the VIR state near the critical point t_{c2}. The width of the peak W becomes narrow exponentially as t approaches to t_{c2}. It can be adequately described using an exponential function $W = C\exp[-A/(V - V_{c2})^{\nu}]$, where the fitting parameters $C = 1.0051$, $A = 1.6344$, and $\nu = 0.470$. Figure 7(b) indicates that the fitting function (solid line) agrees very well with the NRG results (scattering dots). This exponentially-dependent width W indicates that the VIR–OSS transition at t_{c2} is of the KT type.[32] Figures 7(c) and 7(d) present the charge occupation n'_i and the double occupation $\langle n'_{i\uparrow}n'_{i\downarrow}\rangle$ on each orbital for $V = 0.12$ and different t. The abrupt changes in n'_i and $\langle n'_{i\uparrow}n'_{i\downarrow}\rangle$ at the critical point t_{c1} indicate a first order QPT from the CB to the VIR state. From Figs. 7(c) and 7(d), one can easily obtain that the single occupation on the orbital $f_{1\sigma}$ increases from about 0.41 to about 0.58 at the critical point t_{c1}. This feature favors the full conductance in the VIR state as

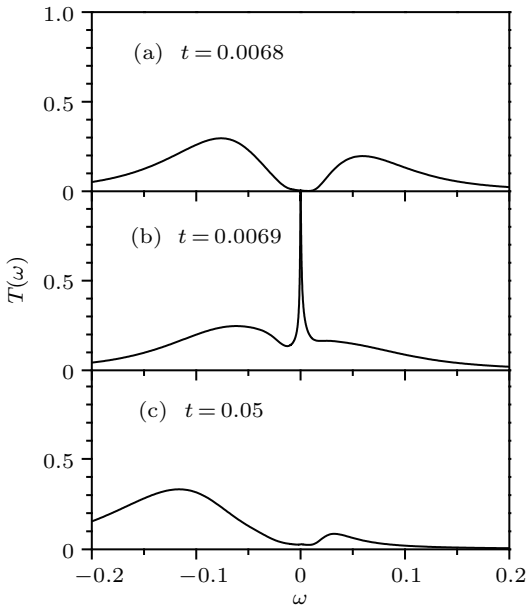


Fig. 6. Transmission coefficient $T(\omega)$ at zero temperature for different t values. Here, $\Gamma = 0.01$, $t_0 = 0.01$, $U = 0.1$, $V = 0.12$, and $\epsilon = -U/2 - 2V$.

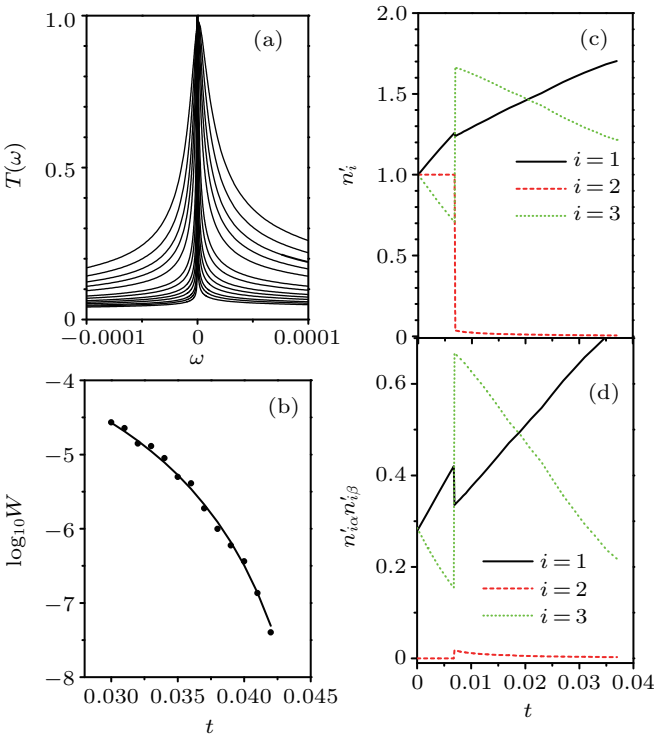


Fig. 7. (color online) (a) Transmission $T(\omega)$ in the VIR state near the critical point $t = t_{c2}$; the curves from top to bottom are for t=0.030 to 0.042 in steps of 0.001. (b) The width of the Kondo peak W (scattering dots) and its stimulant exponential function (solid line) as a function of t near t_{c2}. (c) Charge occupation n'_i and (d) double occupation $\langle n'_{i\uparrow}n'_{i\downarrow}\rangle$ on orbital $f_{i\sigma}$ as a function of t. The remaining parameters are the same as in Fig. 6.

discussed in Section 3.1. In the VIR state and near the critical point t_{c1}, the orbital $f_{2\sigma}$ is nearly empty while the orbital $f_{3\sigma}$ is almost doubly occupied. This feature is somewhat different from that for $t = 0$. In the VIR state without frustration (e.g., $t = 0$ and $V > V_{c2}$ in Fig. 4(c)), the possibility of being doubly occupied on the orbital $f_{2\sigma}$ is the same as that of being empty due to the particle–hole symmetry. However, the orbital $f_{2\sigma}$ is nearly empty due to the frustration t in Fig. 7(c). The common feature for $t = 0$ and $t \neq 0$ is that the increase of the single occupation on the orbital $f_{1\sigma}$ induces the full conductance in the VIR state. As t increases continuously in the regime $t > t_{c1}$, the charge occupation and the double occupation on the orbital $f_{1\sigma}$ increases continuously. As $t > t_{c2}$, the system transits to the OSS state through a QPT of the KT type.

4. Conclusion

We have demonstrated that in a triangular TQD system with two dots connected to leads, the QPT can be characterized by the transmission. The interplay between the on-site Hubbard repulsion U, the interdot Coulomb repulsion V, and the frustration t results in a complicated phase diagram. In case of $t = 0$, the system is particle–hole symmetric at half-filling. For small V, each dot is singly occupied due to the Hubbard interaction U and the TQD forms a spin doublet, which is screened by the metallic leads and is accompanied with the Kondo resonance at low temperature. With the increase of V, the system undergoes a KT transition to the CB state at $V = V_{c1}$ and a first order transition to the VIR state at $V = V_{c2}$. As the interdot hopping t is turned on, the particle–hole symmetry is broken and the system is frustrated. For small V, with the increase of t, there exists a first order transition from the KR state to the OSS state, in which the even orbital is doubly occupied and forms an orbital spin singlet. For larger V, with increasing t, we find the CB–VIR transition of first order at t_{c1} and the VIR–OSS transition of the KT type at t_{c2}.

The phase boundary can be characterized by the transmission spectra $T(\omega)$. For instance, at the KR–OSS transition point, the Kondo resonance peak disappears on the side of the OSS state. Along the two KT transition lines, the width of the transmission peak depends exponentially on the distance to the critical point. In the CB regime, we observe two CB peaks, while in the VIR state the transmission with unitary limit recovers. Since the transmission can be conveniently obtained by the experiment, we believe this characteristic provides a possibility to experimentally demonstrate the QPT in a TQD system.

References

[1] Cornaglia P S and Grempel D R 2005 *Phys. Rev. B* **71** 075305
[2] Dias da Silva L G G V, Sandler N P, Ingersent K and Ulloa S E 2006 *Phys. Rev. Lett.* **97** 096603
[3] Mravlje J, Ramsak A and Rejec T 2006 *Phys. Rev. B* **73** 241305
[4] Logan D E, Wright C J, and Galpin M R 2009 *Phys. Rev. B* **80** 125117
[5] Chung C H, Zarand G, and Wolfle P 2008 *Phys. Rev. B* **77** 035120
[6] Kuzmenko T, Kikoin K and Avishai Y 2006 *Phys. Rev. Lett.* **96** 046601
[7] Kuzmenko T, Kikoin K and Avishai Y 2006 *Phys. Rev. B* **73** 235310
[8] Žitko R and Bonca J 2007 *Phys. Rev. Lett.* **98** 047203
[9] Ingersent K, Ludwig A W W and Affleck I 2005 *Phys. Rev. Lett.* **95** 257204
[10] Mitchell A K and Logan D E 2010 *Phys. Rev. B* **81** 075126
[11] Mitchell A K, Jarrold T F and Logan D E 2009 *Phys. Rev. B* **79** 085124
[12] Vernek E, Orellana P A, and Ulloa S E 2010 *Phys. Rev. B* **82** 165304
[13] Wang W Z 2007 *Phys. Rev. B* **76** 115114.
[14] Xiong Y C, Zhang J, Zhou W H and Laref A 2017 *Chin. Phys. B* **26** 097102
[15] Chen J C, Chang A M and Melloch M R 2004 *Phys. Rev. Lett.* **92** 176801
[16] Roch N, Florens S, Bouchiat V, Wernsdorfer W and Balestro F 2008 *Nature* **453** 633
[17] Gaudreau L, Studenikin S A, Sachrajda A S, Zawadzki P, Kam A, Lapointe J, Korkusinski M and Hawrylak P 2006 *Phys. Rev. Lett.* **97** 036807
[18] Rogge M C and Haug R J 2008 *Phys. Rev. B* **77** 193306
[19] Amaha S, Hatano T, Kubo T, Teraoka S, Tokura T, Tarucha S and Austing D G 2009 *Appl. Phys. Lett.* **94** 092103
[20] Cockins L, Miyahara Y, Bennett S D, Clerk A A, Studenikin S, Poole P, Sachrajda A and Grutter P 2010 *PNAS* **107** 9496
[21] Pierre M, Wacquez R, Roche B, Jehl X, Sanquer M, Vinet M, Prati E, Belli M and Fanciulli M 2009 *Appl. Phys. Lett.* **95** 242107
[22] Granger G, Gaudreau L, Kam A, Pioro-Ladri'ere M, Studenikin S A, Wasilewski Z R, Zawadzki P and Sachrajda A S 2010 *Phys. Rev. B* **82** 075304
[23] Amaha S, Hatano T, Tamura H, Teraoka S, Kubo T, Tokura Y, Austing D G and Tarucha S 2012 *Phys. Rev. B* **85** 081301(R)
[24] Žitko R and Bonca J 2008 *Phys. Rev. B* **77** 245112
[25] Mitchell A K and Logan D E 2010 *Phys. Rev. B* **81** 075126
[26] Mitchell A K, Jarrold T F and Logan D E 2009 *Phys. Rev. B* **79** 085124
[27] Numata T, Nisikawa Y, Oguri A and Hewson A C 2009 *Phys. Rev. B* **80** 155330
[28] Oguri A, Amaha S, Nishikawa Y, Numata T, Shimamoto M, Hewson A C and Tarucha S 2011 *Phys. Rev. B* **83** 205304
[29] Vernek E, Büsser C A, Martins G B, Anda E V, Sandler N and Ulloa S E 2009 *Phys. Rev. B* **80** 035119
[30] Krishna-murthy H R, Wilkins J W and Wilson K G 1980 *Phys. Rev. B* **21** 1003
[31] Krishna-murthy H R, Wilkins J W and Wilson K G 1980 *Phys. Rev. B* **21** 1044
[32] Hofstetter W 2000 *Phys. Rev. Lett.* **85** 1508
[33] Hofstetter W and Schoeller H 2001 *Phys. Rev. Lett.* **88** 016803